Acta Crystallographica Section F
Structural Biology and Crystallization Communications
ISSN 1744-3091

Cloning, purification, crystallization and preliminary crystallographic analysis of a ribokinase from *Staphylococcus aureus*

Lin Wang,[a,b] Haipeng Wang,[a] Jianbin Ruan,[a] Changlin Tian,[a,b] Baolin Sun[a,b] and Jianye Zang[a]*

[a]School of Life Sciences, University of Science and Technology of China, 96 Jinzhai Road, Hefei, Anhui 230027, People's Republic of China, and [b]Hefei National Laboratory for Physical Sciences at Microscale, University of Science and Technology of China, 96 Jinzhai Road, Hefei, Anhui 230027, People's Republic of China

Correspondence e-mail: zangjy@ustc.edu.cn

Received 18 March 2009
Accepted 21 April 2009

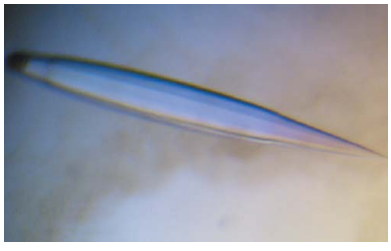

The gene SA239 from *Staphylococcus aureus* encodes a ribokinase that catalyzes the phosphorylation of D-ribose to produce ribose-5-phosphate. Sa239 was crystallized using the hanging-drop vapour-diffusion method. The crystals diffracted to 2.9 Å resolution and belonged to space group $P6_122$ or $P6_522$, with unit-cell parameters $a = b = 91.8$, $c = 160.7$ Å. Preliminary crystallographic analysis revealed that the Matthews coefficient V_M was 3.01 Å^3 Da^{-1}, indicating the presence of one molecule in the asymmetric unit.

1. Introduction

D-Ribose is one of the most important sugars that widely exist in biological systems and can be used in the synthesis of nucleotides, histidine and tryptophan or for energy production. After uptake into the cytoplasm of the cell, D-ribose is phosphorylated by ribokinase and the product, ribose-5-phosphate, then enters the metabolic pathways. Ribokinase also plays a key role in the recycling of sugars produced from the metabolism of nucleotides (Anderson & Cooper, 1969; Lopilato *et al.*, 1984). Sequence alignment revealed that ribokinase belongs to the PfkB carbohydrate kinase family and is found in both prokaryotes and eukaryotes (Bork *et al.*, 1993).

Ribokinase catalyzes the reaction of D-ribose and ATP to produce ribose-5-phosphate and ADP. The catalytic reactivity of ribokinase is activated by the divalent cation Mg^{2+}. Other metal ions such as Mn^{2+}, Co^{2+}, Ca^{2+}, Ni^{2+} and Cu^{2+} can replace Mg^{2+} to satisfy the divalent-cation requirement of ribokinase. In the absence of these metal ions, ribokinase loses its catalytic ability (Chuvikovsky *et al.*, 2006). Monovalent cations such as K^+ or Cs^+ are also needed for the activation of ribokinase. The activation mechanism of monovalent cations has been elucidated from the crystal structure of ribokinase from *Escherichia coli* in complex with caesium, in which the ion binds between two loops adjacent to the active site and assists in the formation of the anion hole that functions to stabilize the intermediates of the catalytic reaction (Andersson & Mowbray, 2002).

The catalytic activity of ribokinase is nearly completely dependent on the presence of pentavalent ions (PIV) such as phosphate. This property was first demonstrated with the ribokinase from *E. coli*. Adding inorganic phosphate ions to the reaction system caused an increase in the maximum velocity and a decrease in the K_m for D-ribose. Other PIV such as arsenate and vanadate had the same effect as phosphate (Maj & Gupta, 2001). Although a phosphate ion is present near the active site in the structure of *E. coli* ribokinase in complex with ribose and ADP (Sigrell *et al.*, 1998), the exact role that PIV play in activating ribokinase still remains elusive. In order to address this question, Sa239 from *Staphylococcus aureus* was cloned, expressed and purified and the ribokinase activity of Sa239 was characterized (data not shown). Crystallization trials of Sa239 were carried out.

2. Materials and methods

2.1. Cloning, overexpression and purification

The Sa239 gene (accession No. NC_007795.1) was amplified by polymerase chain reaction (PCR) from the genomic DNA of *S. aureus*

using the oligonucleotide primers 5′-CGACGACGACATATGATG-ACCAACAAAGTTGTTATTTTAG (forward) and 5′-GACCTCG-AGTTAAACTTGATTTACTTCTTCTAGTAG (reverse) (purchased from Sangon). The PCR product was digested with *Nde*I and *Xho*I and cloned into the PET-23b vector (Novagen) with a SUMO protein fused at the N-terminus after the His_6 tag. The resulting plasmid was confirmed by DNA-sequence analysis of the inserted ORF of Sa239 (Amphipound Biotech).

The SUMO-Sa239 fusion protein was expressed in *E. coli* BL21 (DE3) cells (Novagen). Cells containing the target plasmid were grown in Luria–Bertani (LB) medium supplemented with 0.4 µg ml^{-1} ampicillin at 310 K until the $OD_{600\,nm}$ reached 0.6; they were then induced with 0.4 m*M* isopropyl β-D-1-thiogalactopyranoside (IPTG) and grown for a further 20 h at 293 K. The cells were harvested by centrifugation at 6000*g* for 8 min at 277 K and the resulting bacterial pellets were resuspended in lysis buffer (500 m*M* NaCl, 5% glycerol, 25 m*M* Tris–HCl pH 8.0). After cell lysis by ultrasonication on ice, the lysate was clarified by centrifugation at 15 000*g* for 30 min at 277 K. The supernatant was loaded onto an Ni–NTA nickel-chelating column (Qiagen) pre-equilibrated with lysis buffer. The column was washed with 20 column volumes of washing buffer (500 m*M* NaCl, 5% glycerol, 25 m*M* Tris–HCl, 20 m*M* imidazole pH 8.0) to remove the contaminant and the target protein was eluted with elution buffer (500 m*M* NaCl, 5% glycerol, 25 m*M* Tris–HCl, 500 m*M* imidazole pH 8.0). The eluate was exchanged into digestion buffer (150 m*M* NaCl, 1 m*M* DTT, 1 m*M* EDTA, 25 m*M* Tris–HCl pH 8.0) using a PD-10 desalting column (GE Healthcare) pre-equilibrated with the same buffer and subjected to SUMO protease cleavage for 10 h at 277 K. The cleaved protein mixture was passed through an Ni–NTA nickel-chelating column pre-equilibrated with lysis buffer. The flowthrough fraction was loaded onto a HiLoad 16/60 Superdex 200 size-exclusion column (GE Healthcare) pre-equilibrated with column buffer (150 m*M* NaCl, 25 m*M* Tris–HCl pH 8.0). The eluted fraction that contained the target protein was concentrated by centrifugal ultrafiltration (Millipore, 5 kDa cutoff) to 8.0 mg ml^{-1} for further use. All purification steps were performed at 277 K and the result of each step was monitored by SDS–PAGE.

2.2. Crystallization

Crystallization experiments were set up by hand using the hanging-drop vapour-diffusion method at 295 K in 48-well plates (XtalQuest Co.). Crystal Screen, Crystal Screen II (Hampton Research), Wizard I and Wizard II (Emerald Biosystems) were used for the initial crystallization condition screen. 1 µl protein solution (8.0 mg ml^{-1} in buffer containing 150 m*M* NaCl, 25 m*M* Tris–HCl pH 8.0) was mixed with 1 µl well solution and the mixture was equilibrated over 500 µl well solution. Microcrystals appeared in several days in one of the 194 initial screening conditions. Optimization was carried out by changing the pH of the buffer and the precipitant concentration. After several rounds of refinement, a well diffracting single crystal was obtained. The crystallization conditions of Sa239 in complex with phosphate were screened using the same procedure.

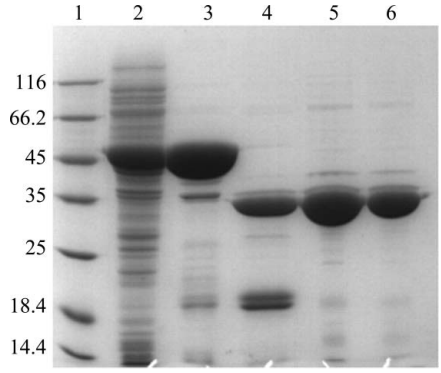

Figure 1
SDS–PAGE analysis of the purification of Sa239. Lane 1, markers (kDa); lane 2, cell lysate; lane 3, eluant from Ni–NTA nickel-chelating column; lane 4, SUMO-Sa239 cleaved by SUMO protease; lane 5: the flowthrough fraction after passage of the SA239 and SUMO mixture through the second Ni–NTA nickel-chelating column; lane 6: eluted fraction containing Sa239 from the HiLoad 16/60 Superdex 200 size-exclusion column.

Table 1
Crystal parameters and data-collection statistics for the Sa239 crystal.

Values in parentheses are for the highest resolution shell.

Space group	$P6_122$ or $P6_522$
Unit-cell parameters (Å, °)	$a = b = 91.8$, $c = 160.7$, $\alpha = \beta = 90$, $\gamma = 120$
Resolution (Å)	50–2.89 (2.94–2.89)
Unique reflections	9555
Redundancy	13.5 (10.5)
Average $I/\sigma(I)$	17.5 (2.4)
Completeness (%)	100 (99.8)
R_{merge}† (%)	10.2 (40.6)

† $R_{merge} = \sum_{hkl}\sum_i |I_i(hkl) - \langle I(hkl)\rangle| / \sum_{hkl}\sum_i I_i(hkl)$, where $I_i(hkl)$ is the ith observation of reflection hkl and $\langle I(hkl)\rangle$ is the weighted average intensity of all observations i of reflection hkl.

2.3. Diffraction data collection and processing

The crystal of Sa239 was harvested and soaked in a cryoprotectant solution containing 35%(*w*/*v*) PEG 3000, 0.1 *M* sodium citrate pH 5.6 for several seconds. The crystal was then flash-cooled and subjected to X-ray diffraction data collection at 100 K on synchrotron-radiation beamline 3W1A at BSRF (Beijing). A complete diffraction data set containing 180 diffraction images was collected from one crystal with an oscillation angle of 1° per image. Diffraction data were indexed, integrated and scaled using *HKL*-2000 (Otwinowski & Minor, 1997). Data-collection and processing statistics are listed in Table 1.

3. Results and discussion

About 2 mg of Sa239 could be purified from 5 g of wet cell pellet and the purity of Sa239 was more than 95% as monitored by SDS–PAGE (Fig. 1). The purified Sa239 was concentrated to 8 mg ml^{-1} for crystal screening experiments. Several days after the crystallization experiments had been set up, a microcrystal was obtained from a condition

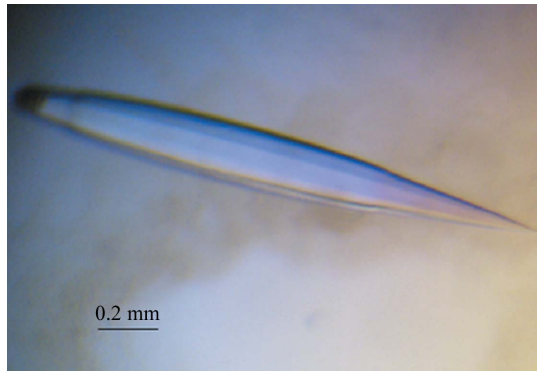

Figure 2
Crystal of Sa239.

Figure 3
X-ray diffraction frame collected from a crystal of Sa239.

containing 20%(*w*/*v*) PEG 3000, 0.1 *M* sodium citrate pH 5.6. The crystal obtained using this condition was small and was not suitable for X-ray data collection. The initial conditions were optimized in order to yield crystals suitable for X-ray diffraction. After several rounds of refinement, large crystals appeared at 295 K in conditions consisting of 23%(*w*/*v*) PEG 3000, 0.1 *M* sodium citrate pH 5.6. Typical crystal dimensions were 0.15 × 0.10 × 0.75 mm (Fig. 2). The crystal was flash-cooled and X-ray diffraction data were collected at 100 K on beamline 3W1A at BSRF. The crystal diffracted X-rays to 2.9 Å resolution. One of the diffraction images is shown in Fig. 3 and the statistics of data collection and processing are summarized in Table 1. The crystal belonged to the hexagonal space group $P6_122$ or $P6_522$. The calculated Matthews coefficient (V_M) of 3.01 Å^3 Da^{-1}, with a solvent content of 59.20%, indicated the presence of one molecule in the asymmetric unit (Matthews, 1968).

The structure of Sa239 will be solved by the molecular-replacement method. Microcrystals of Sa239 in complex with phosphate were obtained at 295 K using a protein concentration of 8.0 mg ml^{-1} and a reservoir solution comprising 10 m*M* sodium phosphate, 22%(*w*/*v*) PEG 3000, 0.1 *M* sodium citrate pH 5.6. The crystals are presently not large enough for diffraction and further optimization is ongoing. The structure of Sa239 and of its complex with phosphate ions will help in elucidating the mechanism by which phosphate ions activate ribokinase.

We thank Drs Yuhui Dong and Zengqiang Gao for assistance with data collection on beamline 3W1A of the Beijing Synchrotron Radiation Facility at the Institute of High Energy Physics, Chinese Academy of Sciences. This work was supported by a grant from the Chinese Ministry of Health (No. 2008ZX10003-006-2) to JZ and BS, and grants from the Chinese Ministry of Science and Technology (Nos. 2006CB806501 and 2009CB825502 to JZ and No. 2007-CB914304 to CT).

References

Anderson, A. & Cooper, R. A. (1969). *Biochim. Biophys. Acta*, **177**, 163–165.
Andersson, C. E. & Mowbray, S. L. (2002). *J. Mol. Biol.* **315**, 409–419.
Bork, O., Sander, C. & Valencia, A. (1993). *Protein Sci.* **2**, 31–40.
Chuvikovsky, D. V., Esipov, R. S., Skoblov, Y. S., Chupova, L. A., Muravyova, T. I., Miroshnikov, A. I., Lapinjoki, S. & Mikhailopulo, I. A. (2006). *Bioorg. Med. Chem.* **14**, 6327–6332.
Lopilato, J. E., Garwin, J. L., Emr, S. D., Silhavy, T. J. & Beckwith, J. R. (1984). *J. Bacteriol.* **158**, 665–673.
Maj, M. C. & Gupta, R. S. (2001). *J. Protein Chem.* **20**, 139–144.
Matthews, B. W. (1968). *J. Mol. Biol.* **33**, 491–497.
Otwinowski, Z. & Minor, W. (1997). *Methods Enzymol.* **276**, 307–326.
Sigrell, J. A., Cameron, A. D., Jones, T. A. & Mowbray, S. L. (1998). *Structure*, **6**, 183–193.